Publications of the Astronomical Society of Japan Advance Access published July 16, 2014

Publ. Astron. Soc. Japan (2014) 00 (0), 1–6
doi: 10.1093/pasj/psu059
Advance Access Publication Date: 2014 0

Rotation Curve Anomaly and Galactic Warp in M 51

Shouta OIKAWA[1,*] and Yoshiaki SOFUE[1,2,†,‡]

[1]Department of Physics, 2-1-1 Hodokubo, Meisei University, Hino-shi, Tokyo 191-0052
[2]Institute of Astronomy, The University of Tokyo, 2-21-1 Osawa, Mitaka, Tokyo 181-0015

[‡]E-mail: sofue@ioa.s.u-tokyo.ac.jp

Received 2013 July 3; Accepted 2014 May 19

Abstract

We revisit the anomaly of rotation curve in the nearly face-on galaxy M 51 that shows an apparently faster decrease of rotation velocity than the Keplerian law in the outer disk, further showing apparent counter rotation in the outermost H I disk. We interpreted this anomaly as being due to warping of the galactic disk, and determined the warping structure of M 51's disk using the tilted-ring method, while assuming that the intrinsic rotation curve is normal. It has been shown that the disk is nearly flat in the inner disk at a constant inclination angle, but the disk suddenly bends at radius 7.5 kpc by about 27°. The inclination angle, then, decreases monotonically outward, reaching a perfect face-on ring at 18 kpc, beyond which the disk is warped in the opposite sense to the inner disk, resulting in apparent counter rotation.

Key words: galaxies: individual (M 51) — galaxies: general — galaxies: kinematics and dynamics — galaxies: structure

1 Introduction

Spiral galaxies have universally flat rotation curves (Rubin et al. 1980; Persic et al. 1996; Sofue & Rubin 2001; Salucci et al. 2007). However, two exceptional cases of an anomalously rapid decrease in the rotation velocity have been known: one in the edge-on peculiar galaxy M 82 (NGC 3032) and the other in the face-on Sc spiral M 51 (NGC 5194).

It was shown that the rotation curve of M 82 could be fitted by the Keplerian law at radii beyond ∼ 3 kpc. The Kepler rotation was interpreted as due to absence of a dark halo by tidal truncation during the past gravitational encounter with the parent galaxy M 81 (Sofue 1998). For an edge-on galaxy like M 82, the observed radial velocity can be almost directly converted to rotation velocity for a negligible correction of the inclination, representing the real kinematics of the galactic disk.

On the other hand, the rotation curve for a face-on galaxy is sensitive to the inclination angle. The face-on galaxy M 51 has flat rotation in the inner disk, but the curve suddenly bends at radius 2′.5 (7.5 kpc), and decreases faster than the Keplerian law (Sofue 1996). M 51's rotation curve has been obtained at various wavelengths in order to exhibit high accuracy in optical (Tully 1974), H I (Roberts & Warran 1970; Haynes et al. 1978; Rots et al. 1990; Tilanus & Allen 1991; Rand et al. 1993), and CO line observations (García-Burillo et al. 1993; Nakai et al. 1994; Kuno et al. 1995; Kuno & Nakai 1997; Koda et al. 2011; Shetty et al. 2007). Observations showed that the CO-line rotation curve in the molecular gas disk is nearly flat, whereas H I-line observations showed an apparently decreasing velocity beyond ∼ 8 kpc. Even counter rotation was observed in the outermost H I disk (Appleton et al. 1986; Rots et al. 1990).

*Present address: Ministry of Defence, Shibata, Niigata 957-8530.
†Present address on leave from Meisei University: The University of Tokyo.

In this short note, we revisit the anomaly of the apparent rotation curve of M 51, and interpret it as being due to warping of the disk.

2 Anomalous rotation curve in M 51

2.1 Apparent bend of rotation curve at 7.5 kpc

Figure 1 shows a rotation curve of M 51 obtained by Sofue (1996) from a compilation of observations in the Hα, CO and H I line emissions. The original curve in Sofue (1996) was calculated for an inclination of $i = 20^\circ$, while the curve here has been re-calculated using a more recent inclination value of the inner main disk, $i = 24^\circ$ (Shetty et al. 2007). The rotation curve is nearly flat in the inner disk at $r < 7$ kpc. However, it bends suddenly at $r = 7.5$ kpc, beyond which the velocity decreases faster than the Keplerian law. In figure 2 we compare M 51's curve with those of typical disk galaxies, which exhibit nearly flat rotation until their edges.

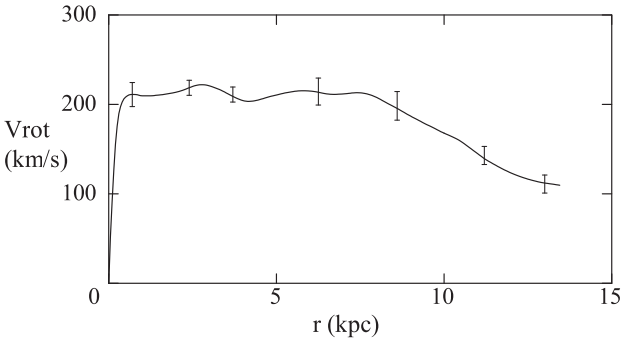

Fig. 1. Observed rotation curve of M 51 obtained for a constant inclination of $i = 24^\circ$ using the data from Sofue (1996, 1997), who used $i = 20^\circ$. Error bars are indicated at representative radii.

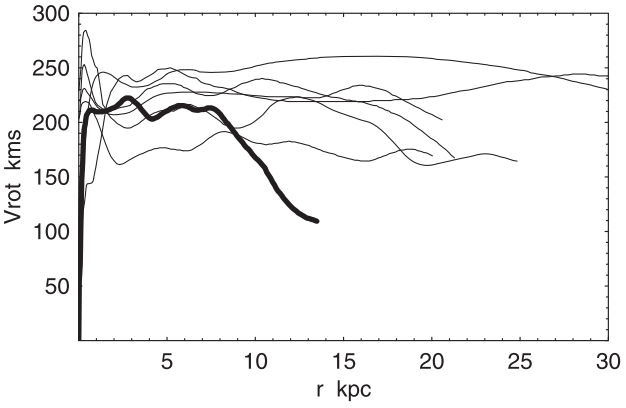

Fig. 2. Rotation curve of M 51 (thick line) compared with rotation curves of the Milky Way, M 31, NGC 891, and NGC 3079 by thin lines (Sofue et al. 1999).

2.2 Counter rotation in the outermost H I disk

The decreasing rotation velocities at larger radii are clearly observed in H I-line velocity fields (Rots et al. 1990; Tillanus & Allen 1990). Using the H I velocity field presented by Rots et al. (1990), we read the contour values of the radial velocities and corresponding radii along the major axis fixed at a position angle of $\phi = 162^\circ$. Thereby, we did not use northern data showing systemic velocities higher than 600 km s^{-1} around the companion galaxy NGC 5195, where H I gas is supposed to be strongly disturbed, except for one point at $r = 10'$ with 580 km s^{-1}. Hence, the northern data are less accurate, while being consistent with the southern measurements.

The measured velocities are shown by small circles (northern half) and triangles (southern half) in figure 3. The values are differences of the radial velocities and the systemic velocity of $V_{\rm sys} = 470$ km s^{-1}, and corrected for the assumed constant inclination angle of $i = 24^\circ$. Rotation velocities were plotted after mirror-rotating superposition of the northern and southern measurements.

The measured values were, then, averaged by a Gaussian-weighted running mean with a half width of 2.5 kpc at every 2.5 kpc radius interval. The obtained rotation velocities are plotted by large dots with error bars in figure 3. H I velocities at $r \lesssim 7$ kpc were not used in the analysis, because of missing H I gas in the inner region.

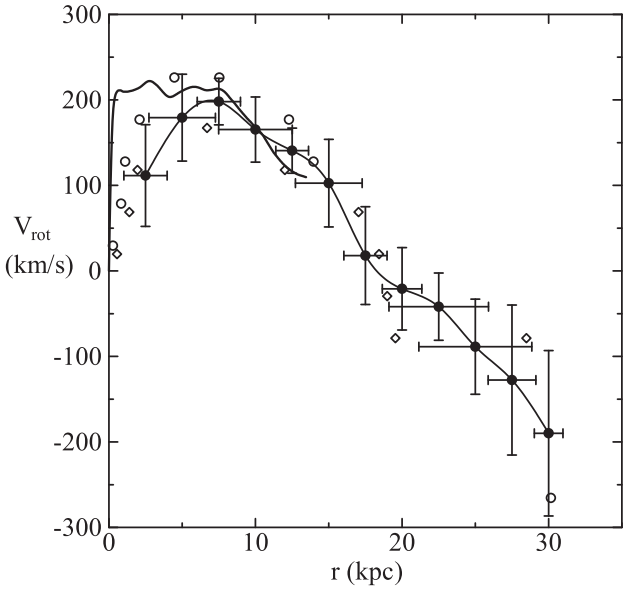

Fig. 3. Apparent H I rotation curve obtained from the contour values in the velocity field by Rots et al. (1990; their figure 7) for a fixed inclination of $i = 24^\circ$and position angle of $\phi = 162^\circ$. The read data are shown by openl circles and diamonds for the northern and southern halves, respectively. Filled circles with error bars are Gaussian-running-averaged rotation velocities with an averaging half width of 2.5 kpc, calculated every 2.5 kpc radius interval. The inserted inner thick line is the rotation curve from figure 1.

Because the number of read data points (contour values) beyond $r \sim 20$ kpc are only one in the northern half and two in the south, the fitted rotation curve at $r > 20$ kpc has a larger uncertainty compared to that within 20 kpc.

The H I rotation curve from $r \sim 7$ kpc to 13 kpc shows a good agreement with those in figure 1. The apparent rotation velocity decreases monotonically up to $r \sim 30$ kpc. It becomes nearly zero at $r \sim 18$ kpc, and further decreases to $\sim -200\,\mathrm{km\,s^{-1}}$ at the measured edge. The bend and monotonical decrease of the rotation curve are observed systematically both in the northern and southern disks. This implies that the anomaly may not be due to local velocity perturbations, but can be attributed to the general kinematics of the whole galactic disk.

3 Tilted-ring method

The rotation velocity, $V_{\rm rot}$, radial velocity, $v_{\rm r}$, and inclination angle, i, in a galactic disk are coupled to each other by

$$v_{\rm r}(r,\theta) = V_{\rm obs}(r,\theta) - V_{\rm sys} = V_{\rm rot}(r)\cos\theta\sin i, \tag{1}$$

where θ is the azimuth angle in the disk of a measured point from the major axis, $V_{\rm obs}(r,\theta)$ is the measured radial velocity and $V_{\rm sys}$ is the systemic velocity of the galaxy. The position angle and the azimuth angle are related by

$$\theta(\phi) = \mathrm{atan}\,(\tan\phi/\cos i)\,. \tag{2}$$

3.1 Simultaneous determination of i and $V_{\rm rot}$

If a velocity field is observed, any coupling of the rotation velocity and the inclination can be solved using the tilted-ring technique (Rogstad et al. 1974; Bosma 1981; Begeman 1989; Józsa et al. 2007). This is due to the functional shape of the variation of $v_{\rm r}(r,\theta)/v_{\rm r}(r,0)$ against the position angle on the sky, ϕ, which is uniquely related to the inclination angle, i, and the azimuth angle, θ. Here, $v_{\rm r}(r,0)$ is the maximum value of $v_{\rm r}$ along an initially chosen ring. The inclination angle i is determined iteratively by comparing the observed and calculated $v_{\rm r}$ variations with ϕ. Once i, and simultaneously $V_{\rm rot} = v_{\rm r}(r,0)/\sin i$, are determined, the same process is applied to the neighboring rings both outward and inward.

This method, called the tilted-ring method, is effective for highly inclined galaxies with large i. However, the functional shape becomes less sensitive to i in face-on galaxies. Begeman (1989) extensively studied the tilted-ring method, and concluded that it is difficult to determine the inclinations for galaxies with inclination angles less than 40°.

3.2 Determination of $V_{\rm rot}$ for given i

If the inclination angle, i, is given by another method, a convenient way to derive a rotation curve is simply to measure the radial velocities along the major axis. The result is not sensitive to the position angle of the major axis according to the above equation's weakly dependency on θ around 0. Given the inclination i, the rotation velocity is obtained by

$$V_{\rm rot} = v_{\rm r}(r,0)/\sin i\,. \tag{3}$$

The inclination angle is often obtained from the major-to-minor axial ratio of isophote contour ellipses on optical images. An alternative way is to compare the integrated H I line width with that expected from the Tully–Fisher relation (Shetty et al. 2007).

However, as equation (3) trivially shows, the error of obtained rotation velocity is large for small i, and the result even diverges for a face-on galaxy with $i \sim 0°$.

3.3 Determination of i for a given $V_{\rm rot}$

Equation (3) is rewritten as $\sin i = v_{\rm r}(r,0)/V_{\rm rot}$, which means that the inclination can be determined by measuring $v_{\rm r}(r,0)$, if $V_{\rm rot}$ is given. This principle is used in the determination of the inclination using the Tully–Fisher relation, where one estimates an intrinsic line width using the disk luminosity, and compares it with the observed line width to obtain the inclination angle. Shetty et al. (2007) obtained $i = 24°$ for M 51 using this method.

The above equation can also be applied to individual annulus rings, if the rotation curve is assumed. It is obvious that the accuracy of determination of i is higher for more face-on galaxies. This method was indeed applied to measure the inclination of the outer H I disk of the face-on galaxy NGC 628 (Kamphuis & Briggs 1992).

4 Determination of inclination for an assumed rotation velocity of M 51

We applied the third application described in the previous section to M 51 to obtain the radial variation of inclination. Following Kuno and Nakai (1997), we defined a universal rotation curve inside 15 kpc radius by Miyamoto–Nagai's (MN) model (Miyamoto & Nagai 1975), and flat rotation at $200\,\mathrm{km\,s^{-1}}$ beyond 15 kpc. Table 1 lists the adopted

Table 1. Miyamoto–Nagai model for M 51.

Component	a_i (kpc)	$M_{\rm s}(M_\odot)$
Bulge	0.35	9.33×10^9
Disk	2.7	6.02×10^{10}
Halo	13.45	1.55×10^{11}

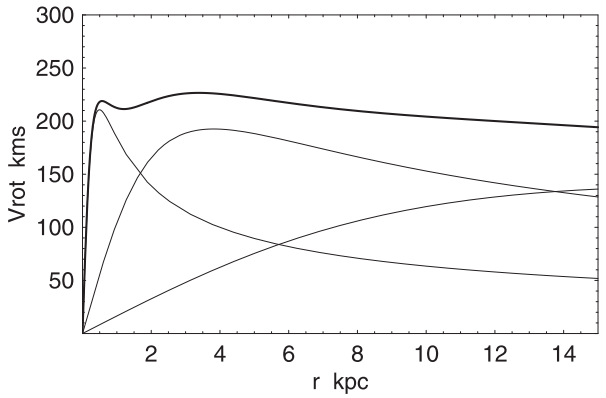

Fig. 4. Assumed rotation curve represented by the MN potential for a non-warped disk, which approximately fits the observation within a radius of 8 kpc for M 51.

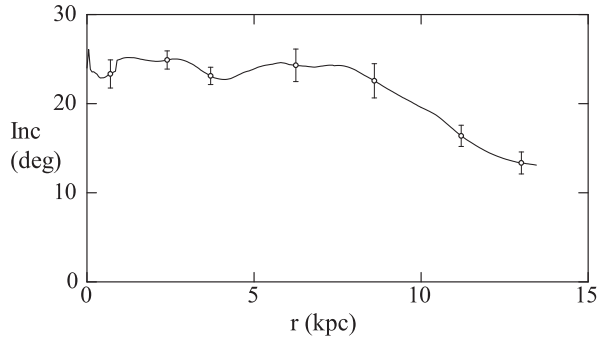

Fig. 5. Variation of the inclination angle of M 51's disk, showing a sudden bend at $r = 7.5$ kpc.

potential parameters for M 51, which approximately reproduce the inner rotation curve at $r < 8$ kpc for a fixed inclination angle of $i = 24°$. Figure 4 shows the adopted rotation curve with these parameters.

Although the nodal position angle weekly affects the result, we adopted the values obtained for the main disk by Shetty et al. (2007), and a fixed value at 162° beyond 8 kpc. We, then, calculated the best-fit inclination angle, i, at each radius with an interval of 0.05 kpc.

Figure 5 shows the thus calculated variation of the inclination angle as a function of the radius. M 51's disk is nearly flat in the inner disk at $r \leq 7$ kpc at $i \simeq 24°$, corresponding to the flat apparent rotation curve. The disk, then, bends suddenly at 7.5 kpc, reaching to an inclination angle of $i \simeq 12°$ at $r = 13$ kpc. The result is weakly dependent on the adopted intrinsic rotation curve, in so far as it is the usual model. Instead of the MN model, we may assume a flat rotation, which is $\pm 10\,\mathrm{km\,s^{-1}}$ different from the MN model in the analyzed region of M 51. This will change in the resulting inclination values by about a few percent.

Figure 6 shows the same, but including the outer H I disk. The warping angle reverses at $r \simeq 18$ kpc, where the galaxy becomes perfectly face on. Beyond this radius, the

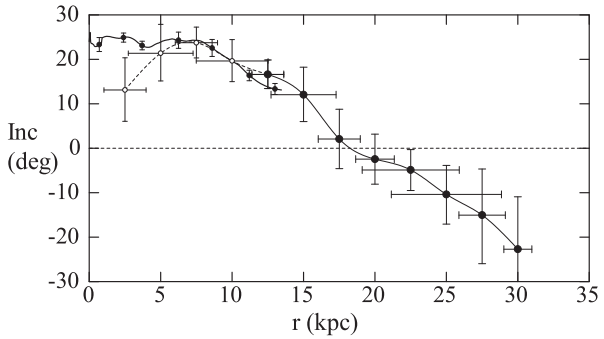

Fig. 6. Inclination angle in the outer H I disk. The disk becomes perfectly face-on ($i = 0°$) at $r = 18$ kpc.

disk is inversely warped, in an opposite sense to the warp of the inner disk. This yielded the apparent counter rotation of the outermost H I disk. Note, however, that the plot at $r > 20$ kpc has a larger uncertainty corresponding to that for the used rotation curve in figure 3.

We comment on the limitation of the accuracy of the outer inclination analysis. The velocity field obtained by Rots et al. (1990) shows that the outer H I disk is not symmetric around the galactic center. Particularly, the velocities around the companion galaxy NGC 5195 are systematically larger than M 51's velocities, and were not used in the present analysis. Nevertheless, the plotted inclination seems to vary smoothly, and the northern and southern values are in agreement with each other.

5 Discussion

We have applied a generalized tilted-ring method to derive an extensive warping structure of M 51 by assuming a universal rotation curve, which may be called the inverse tilted-ring method, a particular method used for face-on galaxies.

5.1 Counter-warping structure of M 51

Figure 7 shows a bird's-eye view of the warped disk of M 51 calculated for the obtained inclinations in the present analysis, shown in figures 5 and 6, as can be seen above from the southern major axis at an altitude of 10°. The inner warping is consistent with a model drawn by Shetty et al. (2007), while the present figure is more quantitative. It is notable that the bending occurs suddenly at $r \sim 7$ kpc, as if the galaxy is broken at this radius. This onset radius of warping corresponds to 0.3 Holmberg radii. which is exceptionally smaller than would be expected from Briggs' (1990) rules. On the other hand, the leading nodal line derived by Shetty et al. (2007) seems to be consistent with the rule.

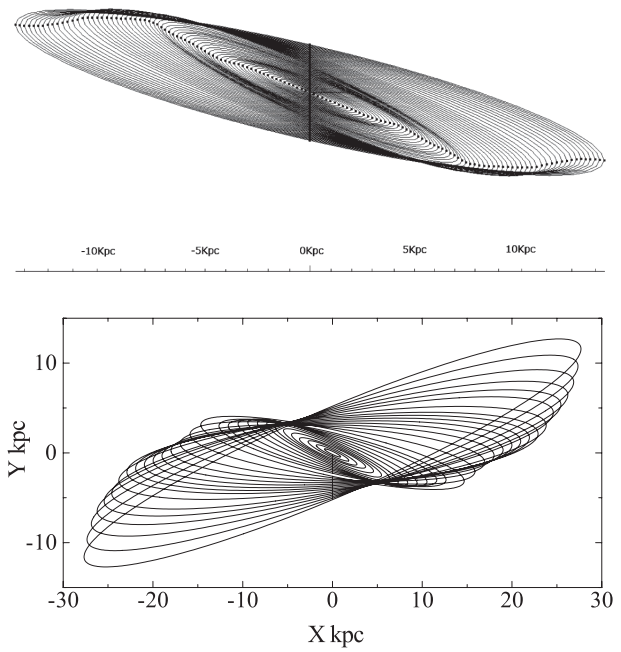

Fig. 7. (Top) Bird's-eye view of tilted rings for the major disk of M 51, as seen from 10° altitude above the southern major axis. (Bottom) Same, but including H I outskirts drawn every 1 kpc by interpolating the obtained inclination values. Note that rings at $r > 20$ kpc are a guess based on less-accurate data, where the H I disk is observed only partially.

The lower panel of figure 7 shows the outermost H I rings. An apparently counter-rotating H I disk, as observed by Appleton, Foster, and Davies (1986) and Rots et al. (1990), is naturally understood by considering a counter warping disk. The inclination of the outermost ring's reaches as large as $i \sim -20°$, or the outermost disk is tilted by $\sim 44°$ from the inner main disk, whose inclination is $i = +24°$. Accordingly, the nearest and farthest parts of the rings are overlapping on the line of sight. Note, however, that rings at $r \gtrsim 20$ kpc are a guess based on an uncertain outermost rotation curve, and the minor axis regions are not detected in the current H I observations.

5.2 Tidal penetration

M 51 is known for its tidal interaction with the companion. The here-obtained warping structure agrees well with a numerical simulation of the tidal interaction of M 51 and NGC 5195 by Dobbs et al. (2011). Both the simulation and the observation show that the disk is bent suddenly at $r \sim 7$ kpc. The observed bending angle, 27°, the angle between the inner and outer disks, agrees with the simulated bending angle, 30°. Hence, the present analysis observationally supports the tidal penetration model of the companion through the main disk at $r \sim 7$ kpc about 120 Myr ago (Dobbs et al. 2011).

5.3 Streaming motion

M 51 is known to have large non-circular streaming motions (Kuno & Nakai 1997; Shetty et al. 2007). However, the observed CO-line position-velocity diagram within the main molecular disk at $r < 7$ kpc looks quite normal, showing a $\pm 20\,\mathrm{km\,s^{-1}}$ deviation from a smooth curve. Hence, the streaming motion, which will appear as a wavy perturbation of rotation velocity, may affect the resulting inclination by ±10% or less.

5.4 Inverse tilted-ring method

The present method is a particular usage of the tilted-ring method, and is applicable to any face-on galaxies. In fact, we applied it to IC 342, and obtained a flat disk at almost a constant inclination corresponding to its quite normal flat rotation curve. The method was also used by Kamphuis and Briggs (1992) to obtain the warping structure in the face-on galaxy NGC 628, where they assumed a constant rotation velocity.

We may be reminded that face-on galaxies with $i \leq 30°$ share $\sim 13\%$ of all galaxies. In these face-on galaxies, the radial velocities yield a large uncertainty in their derived rotation velocity. Instead, if their intrinsic rotation curves can be assumed, the data may be useful for geometrical investigations of galactic disks.

References

Appleton, P. N., Foster, P. A., & Davies, R. D. 1986, MNRAS, 221, 393
Begeman, K. G. 1989, A&A, 223, 47
Bosma, A. 1981, AJ, 86, 1791
Briggs, F. H. 1990, ApJ, 352, 15
Dobbs, C. L., Thesis, C., Pringle, J. E., & Bate, M. R. 2010, MNRAS, 403, 625
García-Burillo, S., Guélin, M., & Cernicharo, J. 1993, A&A, 274, 123
Józsa, G. I. G., Kenn, F., Klein, U., & Oosterloo, T. A. 2007, A&A, 468, 731
Kamphuis, J., & Briggs, F. 1992, A&A, 253, 335
Koda, J., et al. 2011, ApJS, 193, 19
Haynes, M. P., Giovanelli, R., & Burkhead, M. S. 1978, AJ, 83, 938
Miyamoto, M., & Nagai, R. 1975, PASJ, 27, 533
Kuno, N., & Nakai, N. 1997, PASJ, 49, 279
Kuno, N., Nakai, N., Handa, T., & Sofue, Y. 1995, PASJ, 47, 745
Nakai, N., Kuno, N., Handa, T., & Sofue, Y. 1994, PASJ, 46, 527
Persic, M., Salucci, P., & Stel, F. 1996, MNRAS, 281, 27
Rand, R. J. 1993, ApJ, 410, 68
Roberts, M. S., & Warren, J. L. 1970, A&A, 6, 165
Rogstad, D. H., Lockhart, I. A., & Wright, M. C. H. 1974, ApJ, 193, 309
Rots, A. H., Bosma, A., van der Hulst, J. M., Athanassoula, E., & Crane, P. C. 1990, AJ, 100, 387

Rubin, V. C., Ford, W. K., Jr., & Thonnard, N. 1980, ApJ, 238, 471
Salucci, P., Lapi, A., Tonini, C., Gentile, G., Yegorova, I., & Klein, U. 2007, MNRAS, 378, 41
Shetty, R., Vogel, S. N., Ostriker, E. C., & Teuben, P. J. 2007, ApJ, 665, 1138
Sofue, Y., 1996, ApJ, 458, 120
Sofue, Y. 1997, PASJ, 49, 17
Sofue, Y. 1998, PASJ, 50, 227
Sofue, Y., Tutui, Y., Honma, M., Tomita, A., Takamiya, T., Koda, J., & Takeda, Y. 1999, ApJ, 523, 136
Sofue, Y., & Rubin, V. 2001, ARA&A, 39, 137
Tilanus, R. P. J., & Allen, R. J. 1991, A&A, 244, 8
Tully, R. B. 1974, ApJS, 27, 437